



3 4456 0269064 8

ORNL/TM-10603

ornl

**OAK RIDGE
NATIONAL
LABORATORY**

MARTIN MARIETTA

Modeling Heat Generation and Flow in the Advanced Neutron Source Corrosion Test Loop Specimen

R. E. Pawel
D. W. Yarbrough

OAK RIDGE NATIONAL LABORATORY
CENTRAL RESEARCH LIBRARY
CIRCULATION SECTION
4100K FOOT 175
LIBRARY LOAN COPY
DO NOT TRANSFER TO ANOTHER PERSON
If you wish someone else to see this
report, send in name with report and
the library will arrange a loan.

OPERATED BY
MARTIN MARIETTA ENERGY SYSTEMS, INC.
FOR THE UNITED STATES
DEPARTMENT OF ENERGY

Printed in the United States of America. Available from
National Technical Information Service
U.S. Department of Commerce
5285 Port Royal Road, Springfield, Virginia 22161
NTIS price codes—Printed Copy: A03; Microfiche A01

This report was prepared as an account of work sponsored by an agency of the United States Government. Neither the United States Government nor any agency thereof, nor any of their employees, makes any warranty, express or implied, or assumes any legal liability or responsibility for the accuracy, completeness, or usefulness of any information, apparatus, product, or process disclosed, or represents that its use would not infringe privately owned rights. Reference herein to any specific commercial product, process, or service by trade name, trademark, manufacturer, or otherwise, does not necessarily constitute or imply its endorsement, recommendation, or favoring by the United States Government or any agency thereof. The views and opinions of authors expressed herein do not necessarily state or reflect those of the United States Government or any agency thereof.

Metals and Ceramics Division

MODELING HEAT GENERATION AND FLOW IN THE ADVANCED
NEUTRON SOURCE CORROSION TEST LOOP SPECIMEN

R. E. Pawel and D. W. Yarbrough

Date Published - January 1988

NOTICE: This document contains information of
a preliminary nature. It is subject to revision
or correction and therefore does not represent
a final report.

Prepared for the
Office of Basic Energy Sciences
KC 02 02 04 0

Prepared by
OAK RIDGE NATIONAL LABORATORY
Oak Ridge, Tennessee 37831
operated by
MARTIN MARIETTA ENERGY SYSTEMS, INC.
for the
U.S. DEPARTMENT OF ENERGY
under contract DE-AC05-84OR21400



3 4456 0269064 8

CONTENTS

ABSTRACT	1
INTRODUCTION	1
THE MODEL	3
CALCULATIONS	5
APPROXIMATE EQUATIONS	6
RESULTS	13
CONCLUSIONS	15
ACKNOWLEDGMENTS	16
REFERENCES	16

MODELING HEAT GENERATION AND FLOW IN THE ADVANCED
NEUTRON SOURCE CORROSION TEST LOOP SPECIMEN*

R. E. Pawel and D. W. Yarbrough

ABSTRACT

A finite difference computer code HEATING5 was used to model heat generation and flow in a typical experiment envisioned for the Advanced Neutron Source Corrosion Test Loop. The electrical resistivity and thermal conductivity of the test specimen were allowed to vary with local temperature, and the corrosion layer thickness was assigned along the length of the specimen in the manner predicted by the Griess Correlation. The computer solved the two-dimensional transport problem for a given total power dissipated in the specimen and stipulated coolant temperatures and water-side heat-transfer coefficients. The computed specimen temperatures were compared with those calculated on the basis of approximate analytical equations involving the total power dissipation and the assignment of the physical properties based on temperatures at single axial points on the specimen. The comparisons indicate that when temperature variations are large along the axis of the specimen, the variation in local heat flux should not be overlooked when using approximate equations or models. The approximate equations are most accurate near the center of the specimen where the heat flux remains closest to the average value, and in that region the calculated quantities agree closely with the results of the computer code.

INTRODUCTION

The specimen in the Advanced Neutron Source (ANS) Corrosion Test Loop is designed to simulate the heat flow conditions associated with a fuel plate in the proposed reactor. It consists of a 165-mm-long (6.5-in.) aluminum alloy section with a central rectangular channel for coolant flow (Fig. 1). The critical dimensions of the aluminum and the coolant channel

*Research sponsored by the Division of Materials Sciences, U.S. Department of Energy under Contract DE-AC05-84OR21400 with the Martin Marietta Energy Systems, Inc.

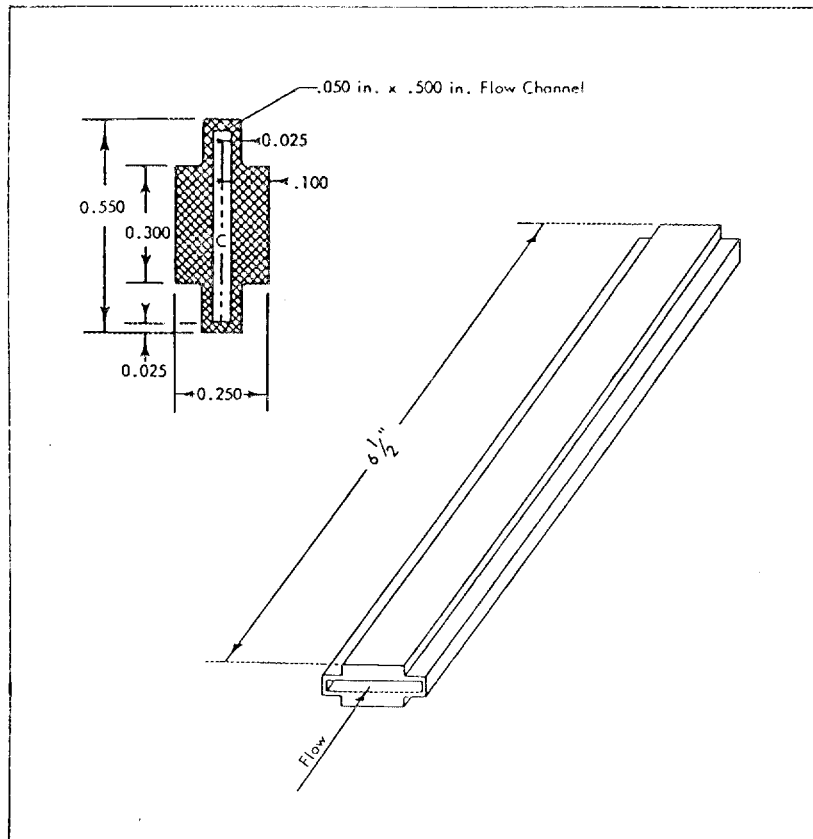


Fig. 1. Sketch of ANS Corrosion Loop Test specimen showing shape and dimensions (1 in. = 25.4 mm). Eighty percent of the heat is generated in the thick part of the specimen wall, and it is one of these thick-walled sections, with its share of the coolant channel, that defines the segment on which the modeling analysis is based.

in the specimen are equivalent to those found in the High Flux Isotope Reactor (HFIR) and the ANS so that the corrosion tests may be run under conditions that approach those of the reactors.

The specimen will be heated by passing large electrical currents (dc) through its length; and, as is the case in an operating reactor, the heat is removed by the rapid flow of cooling water in the rectangular channel. The efficiency of this heat-removal process is the focus of the present investigation. In particular, the development of corrosion product layers, their influence on heat flow, and the means to prevent their formation or to lessen their effect will be studied.

A typical ANS Corrosion Test Loop experiment will involve exposure of the specimen to carefully controlled resistance heating and cooling water flow conditions for up to about 350 h. During this time, the outer surface temperature of the specimen at several points along its length will be monitored to determine the added resistance to heat flow of any growing corrosion product. Therefore, for a typical experiment, we anticipate that the temperature will vary as a function of position along the specimen in the direction of water flow, across the specimen in the direction of heat flow, and with time if a low thermal conductivity corrosion product develops. In addition, the rate of growth of the corrosion product will itself be a function of temperature, so that the gradients in specimen temperature will also change with time.

The significant physical properties of electrical resistivity ρ and thermal conductivity k of aluminum alloys change appreciably with temperature in the range of importance here, and thus both the level of heat generation (via resistance heating) and cooling will vary accordingly. Clearly if the average energy dissipated in the whole specimen is maintained constant over the duration of a test, the local heat generation rates and the local temperature profiles will change in response to the changing temperatures. Such changes are difficult to accommodate accurately in the calculations to determine the various parameters of interest. For example, data obtained in the HFIR test loop¹ were treated according to the following simplifying assumption: the electrical and thermal properties throughout the thickness of the specimen at any point along its length were determined by the temperature of the outside surface of the specimen at that point. Thus, while axial variations in temperature were taken into consideration, the above assumption essentially reduced the computational problem to one of unidirectional heat flow in a locally homogeneous slab in which heat was uniformly generated.

THE MODEL

Because of the possibility of larger temperature gradients for the present experiments, a test of the accuracy of the above simplifying assumption was undertaken through a computer modeling of the corrosion test specimen. The maximum heat flux across the ANS test specimens will

be about 20 MW/m², more than three times that utilized in the HFIR tests. The HEATING5 computer code² was used to perform a two-dimensional heat flow analysis of an appropriate segment geometry defining the active part of the specimen, a strip of aluminum alloy 7.6 mm wide, 2.5 mm thick, and 165 mm long with coolant passing along one surface as shown in Fig. 2. To account for the temperature variation of the physical properties, we divided the specimen segment into 9 zones: 3 axial by 3 lateral; the corrosion product layer was divided into 12 axial zones because its thickness varies significantly with temperature, which increases in the direction of coolant flow. Properties were assigned according to the temperature at the center of each zone, and the steady-state heat transfer solutions were iterated until satisfactory agreement was obtained between the assigned and computed temperatures. The physical properties were assigned on the basis of the data of Tye et al.³ for 6061-T651 aluminum as follows:

$$k = 156.93 + 0.18738T - (2.5238 \times 10^{-4})T^2, \quad (1)$$

$$\rho = 3.90 + 0.0110T, \quad (2)$$

where

k = thermal conductivity of 6061-T651 Al (W/m·K),

ρ = electrical resistivity of 6061-T651 Al ($\Omega\text{-m} \times 10^{-8}$),

T = temperature ($^{\circ}\text{C}$).

The thermal conductivity of the corrosion product was assigned a constant value of 2.25 W/m·K as found by Griess et al.^{1,4} for boehmite ($\text{Al}_2\text{O}_3 \cdot \text{H}_2\text{O}$).

The model specimen was assumed to be cooled by a stream of water passing along its length in contact with the 7.6-- by 135-mm surface. An adiabatic wall was placed on the opposite surface and on each end. The water temperature was assumed to increase uniformly from 65 $^{\circ}\text{C}$ at the inlet to 90 $^{\circ}\text{C}$ at the outlet. The assumption of a linear temperature gradient in the flow direction was also invoked in the HFIR calculations.¹

The water-side heat transfer coefficient was calculated using the average value of the heat flux for the experiment, arbitrarily allowing for

a 70°C temperature drop across the fluid film. For this experiment, an average flux of 15.9 MW/m² (on the basis of 20 kW generated in the specimen segment) was assumed. Thus,

$$h = \bar{Q} / \Delta\bar{T}_f, \quad (3)$$

where

- h = heat transfer coefficient (W/m²·K),
- \bar{Q} = average heat flux from heat transfer surface (W/m²),
- $\Delta\bar{T}_f$ = average temperature drop across fluid film, assigned as 70°C.

The heat transfer coefficient calculated from Eq. (3), $h = 0.227$ MW/m²·K, was then used in the HEATING5 calculations for all conditions regardless of local temperature or heat flux values. Calculations have shown that the actual heat transfer coefficients will probably be smaller than this value, depending sensitively on the coolant velocity and less sensitively on the bulk coolant temperature and heat flux. While the present results, particularly the comparisons between the numerical and analytical calculations, are thought to be virtually unaffected by the assumption of a particular constant heat transfer coefficient, the general effect will be examined in detail at a later date.

CALCULATIONS

The HEATING5 computer program was used to find the steady-state solution to the heat generation and flow problem posed above. After each solution, the calculated temperature at the film-water interface at the midpoint of each of the 12 axial zones was used to assign a thickness to the corrosion product at that zone. A thickness corresponding to 40% of that predicted by the Griess Correlation⁴ for 500 h of exposure was arbitrarily assigned; this assignment provided for reasonable instantaneous film-thickness values having the proper dependence on temperature along the specimen length. In addition, thermal conductivity, electrical resistivity, and the heat generation rate were reassigned to the nine

zones representing the aluminum alloy on the basis of the new temperature distributions. This procedure was followed until a reasonable convergence was apparent. The temperature distributions in the test section at the start of an experiment were also calculated by the HEATING5 program, assuming that only a very thin layer (0.1 μm) of corrosion product existed at that time.

The temperature distributions computed by HEATING5 can be used to obtain estimates of the accuracy of calculated temperatures or parameters based on assumptions made to simplify either the data-gathering or data-treatment processes. Of course, because the computer model is obviously not exact, there are errors in the estimates themselves; however, these effects should be comparatively small.

Schematic diagrams of the initial and final computed temperatures and property values for the specimen for the specified "experimental" conditions are shown in Figs. 2 and 3, where temperature is given in degrees Celsius, thermal conductivity k in watts per meter kelvins, electrical resistivity ρ in ohm meters $\times 10^{-8}$, and local power density G in megawatts per cubic meter. The properties associated with the individual segments of the specimen and corrosion product film are shown in the diagrams, as well as the computed interface temperatures at three points along the axial dimension of the specimen. As noted previously, for purposes of this simulation, the water-side heat transfer coefficient was assumed to be constant and the cooling-water temperature was assumed to vary linearly with position along the specimen. (Other calculations have indicated that the heat transfer coefficient increases along the axis of the specimens, and this might tend to mitigate the interface temperature increases observed along the specimen and lead to a more uniform oxide layer thickness).

APPROXIMATE EQUATIONS

The basic information to be extracted from an experiment in the ANS Corrosion Test Loop will be an estimate of the temperature drop across the growing corrosion product layer due to the local heat flux. Because the experimental data will generally involve only measurements of average heat flux (or total power) in the specimen and temperature measured along

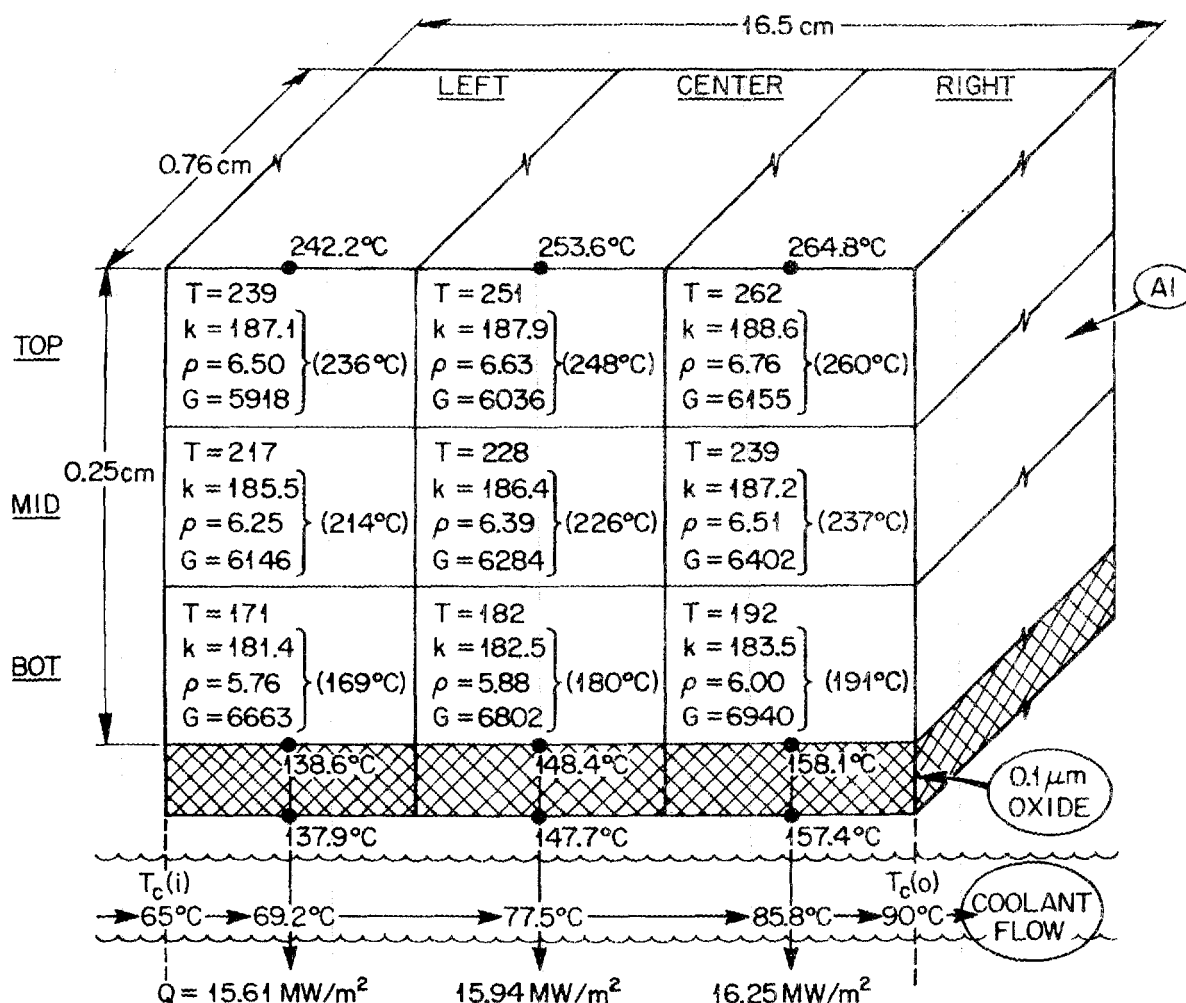


Fig. 2. Schematic diagram of the temperature, physical property, and power generation parameters in sections of model corrosion loop test specimens; (a) Initial (no oxide) and (b) final (oxidized) properties and parameters (oxide thickness assigned as 40% of that predicted by the Griess Correlation for 500 h of operation). Tabulated values refer to the center of each section. Temperatures computed by the HEATING5 code at the three system interfaces for three axial distances along the specimen are also shown (\bullet). Coolant temperatures T_c and heat fluxes Q at the three section midpoints along the specimen are indicated at the bottom of the diagram. Note that even the token oxide film in part (a) ($0.1 \mu\text{m}$) supports almost a 1°C temperature drop at these flux levels. Temperatures shown in parentheses are the penultimate temperatures from which the physical properties of each segment were determined. Thermal conductivity k is given in $\text{W/m}\cdot\text{K}$, electrical resistivity ρ in $\Omega\text{-m} \times 10^{-8}$, and local power density G in MW/m^3 .

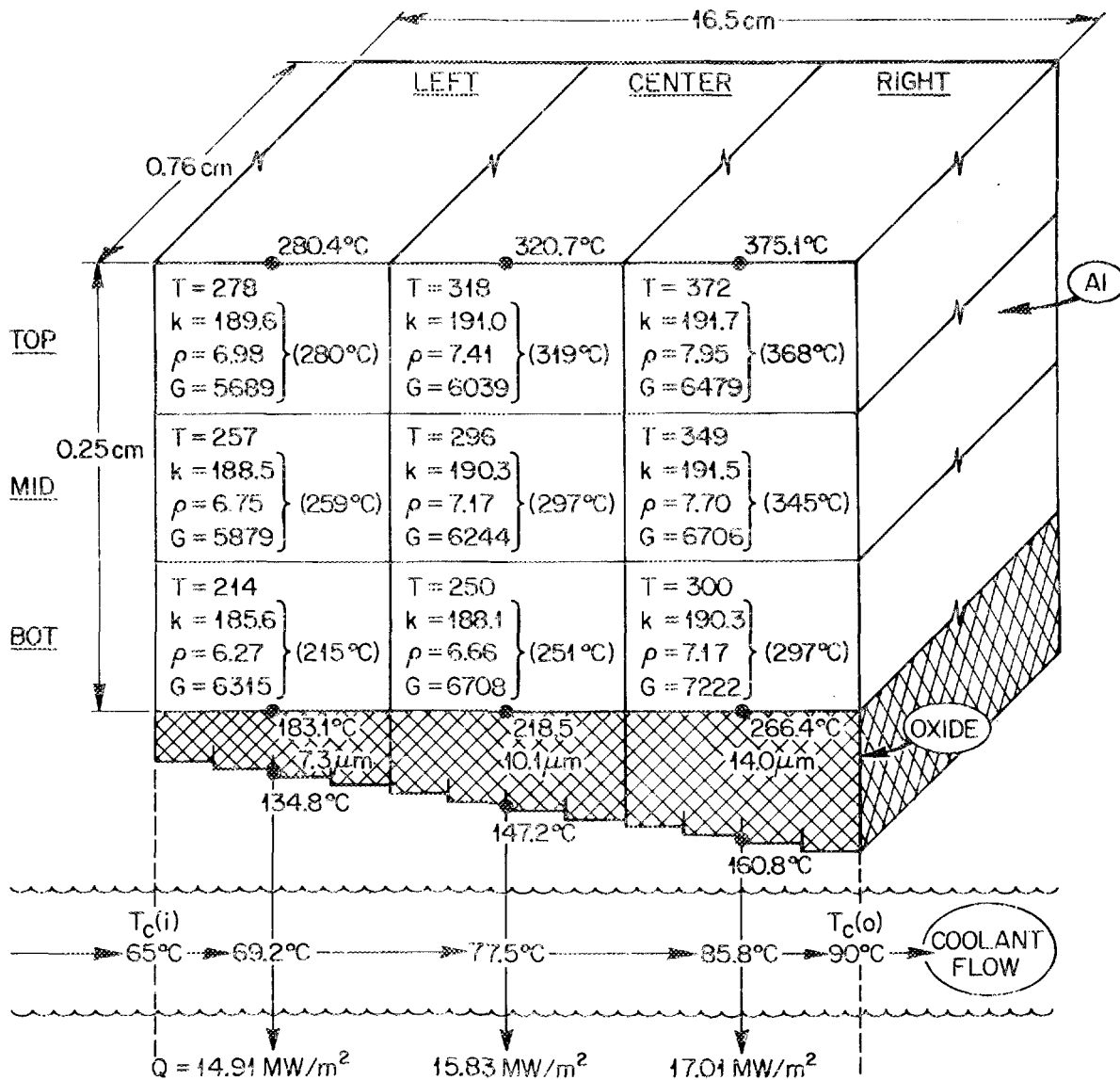


Fig. 3. Schematic diagram of the "final" (oxide thickness assigned as 40% of that predicted by the Griess Correlation for the 500h operation) properties and parameters in the model test specimen following the outline used in Fig. 2. Note the variation in oxide thickness along the length of the test section as well as the variation in heat flux.

the axis on the outer surface of the specimen, the required information must be calculated. It is unlikely that a practical analytical solution to this problem exists, and therefore the present modeling analysis allows comparisons to be made between the commonly used simplified calculations and a more sophisticated finite-difference solution to this heat transfer problem.

A schematic drawing depicting temperatures and temperature differences across the specimen at a given axial location during an experiment is presented in Fig. 4. The following notation is used:

- T_S = temperature at outer surface of aluminum specimen;
- $T_{w/\phi}$ = temperature at interface between specimen and the oxide layer;
- $T_{\phi/c}$ = temperature at interface between oxide layer and coolant;
- T_C = bulk coolant temperature (subscripts i and o refer to inlet and outlet coolant temperatures);
- X_w = specimen wall thickness (2.5 mm);
- X_ϕ = oxide (or corrosion product) layer thickness;
- ΔT_w = temperature drop across specimen wall (calculated on the basis of uniformly generated resistance heating, uniform thermal conductivity, and one-dimensional heat flow);
- Q = heat flow (MW/m^2) across specimen due to resistance heating;
- k_w = average thermal conductivity of specimen wall;
- k_ϕ = average thermal conductivity of oxide layer ($2.25 W/m \cdot K$);
- ΔT_ϕ = temperature drop across oxide layer;
- h = water-side heat transfer coefficient;
- ΔT_f = temperature drop across water film;
- L = length of specimen (165 mm) (x refers to position along specimen length).

The heat generated in the specimen (resistance heating) passes through the oxide layer and into the cooling water. It is assumed that no extraneous heat flows occur. Because of temperature variations along the specimen as well as those brought about by the corrosion process, virtually all of the properties and parameters are functions of position and time.

We envision that an experiment in the ANS Corrosion Test Loop will generally be conducted under conditions where the cooling-water flow rate

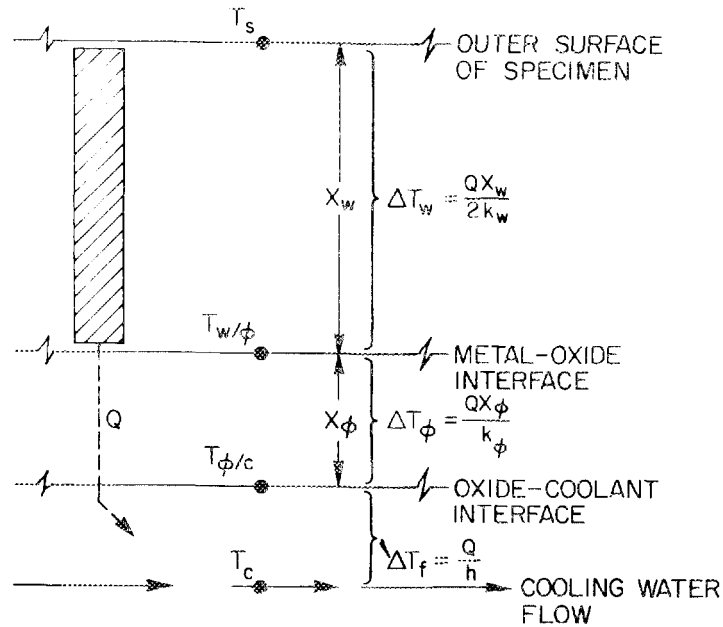


Fig. 4. Schematic drawing illustrating local heat generation and flow in a segment of the corrosion test specimen. The simple equations (assuming uniform properties and one-dimensional heat flow) for the temperature drops across the various layers are given.

and inlet temperature, as well as the average power to the specimen, will be continuously monitored and held constant. Measurements of the outer surface specimen temperature (T_s) will be made at several locations along the axis of the specimen. From these temperature measurements and their changes with time, the temperature drop across the growing oxide film will be calculated. A basic description of the simplified algorithm anticipated for this calculation follows.

I. For each thermocouple position immediately after startup ($t \approx 0$):

1. Measure $T_s(x)$ [at $t = 0$, $T_s = (T_s)_0$]
2. Calculate $Q(x)$

$$Q(x) = [\rho(x)/\bar{\rho}] \bar{Q} , \quad (4)$$

where the average heat flux \bar{Q} equals total power times active power fraction divided by active heat transfer area; total power is calculated from coolant mass flow rate and temperature rise and checked with the electrical input; $\rho(x)$ is property of specimen at $T_s(x)$ [see Eq. (2)]; and $\bar{\rho}$ is average electrical resistivity (i.e., $\Sigma \rho_n/n$).

3. Calculate $T_{w/\phi}$ (at $t = 0$, $T_{w/\phi} = T_{\phi/c}$)

$$T_{w/\phi} = T_{\phi/c} = (T_s)_o - (QX_w/2k_w)_o, \quad (5)$$

where k_w is property of specimen at $T_s(x)$ [see Eq. (1)].
(This equation implies uniform properties and uniform heat generation in specimen.)

4. Calculate T_c

$$T_c(x) \cong T_c(i) + x/L [T_c(o) - T_c(i)]$$

(an iterative or analytical procedure may be used to arrive at a more exact description of the water temperature.)

5. Calculate h

$$h = Q/(T_{\phi/c} - T_c) = Q/[(T_s)_o - QX_w/2k_w - T_c] \quad (7)$$

(and compare with h calculated from dimensional analysis correlations.)

Note: Since T_c should not be a sensitive function of time, assume that $h(x)$ is independent of time.

II. For each thermocouple position during experiment ($t > 0$):

1. Measure $T_s(x)$
2. Calculate $Q(x)$

(as in Step I, using new temperatures to assign properties).

3. Calculate $T_{w/\phi}$ and $T_{\phi/c}$

$$T_{w/\phi} = T_S - QX_w/2k_w , \quad (8)$$

$$T_{\phi/c} = T_C + Q/h , \quad (9)$$

so that

a.

$$\Delta T_\phi = T_{w/\phi} - T_{\phi/c} = T_S - QX_w/2k_w - T_C - Q/h . \quad (10)$$

Previous calculations have invoked the additional assumption that $T_{\phi/c}(x)$ remains constant during an experiment [implying that $Q(x)$, $h(x)$, and $T_C(x)$ also remain constant or vary in a uniquely coordinated manner]. On this basis,

$$T_{\phi/c} = (T_S)_O - (QX_w/2k_w)_O , \quad (11)$$

so that a second approximation for ΔT_ϕ is available:

b.

$$\Delta T_\phi = T_{w/\phi} - T_{\phi/c} = [T_S - QX_w/2k_w] - [(T_S)_O - (QX_w/2k_w)_O] . \quad (12)$$

Finally, if changes in $\Delta T_w(x)$ during an experiment are neglected, then

c.

$$\Delta T_\phi = T_{w/\phi} - T_{\phi/c} = T_S - (T_S)_O . \quad (13)$$

The accuracy of each of these approximations for ΔT_ϕ depends in a complicated way on the manner in which temperature and physical properties of the specimen vary during an experiment. If an experiment is conducted at a constant total power dissipation in the specimen, then we anticipate that at some point near the center, all the approximations (but particularly II.3.b and II.3.c) would exhibit less error.

RESULTS

The objective of the present exercise is to examine the accuracy of particular approximate equations for determining temperature drops across corrosion product layer subject to a heat flux generated in a resistively heated specimen. Many comparisons can be made on the basis of the present computer solution, but only this aspect will be discussed here. Thus, if we assume that we know only the geometry of the test piece, the average power dissipated in the entire specimen, and the inlet cooling water temperature and velocity, the temperature drop across the film can be determined by measuring temperatures on the outer surface of the specimen. Here, we assume that thermocouples 1, 2, and 3 are located at axial positions $L/6$, $3L/6$, and $5L/6$ along the outer surface, as shown in Fig. 2.

Following the above algorithm for each of the three thermocouple positions:

I.1. For $t \cong 0$, "measure" T_S [see Fig. 2, from computer output]:

$$T_{S1} = 242.2^\circ\text{C} \quad T_{S2} = 253.6^\circ\text{C} \quad T_{S3} = 264.8^\circ\text{C}$$

I.2. Using the measured temperatures, we calculate:

$$\begin{array}{lll} \rho_1 = 6.56 \times 10^{-8} \Omega\text{-m} & \rho_2 = 6.69 \times 10^{-8} \Omega\text{-m} & \rho_3 = 6.81 \times 10^{-8} \Omega\text{-m} \\ k_{w1} = 187.5 \text{ W/m}\cdot\text{K} & k_{w2} = 188.2 \text{ W/m}\cdot\text{K} & k_{w3} = 188.9 \text{ W/m}\cdot\text{K} \\ \bar{\rho} = 6.69 \times 10^{-8} \Omega\text{-m} & & \\ Q_1 = 15.59 \text{ MW/m}^2 & Q_2 = 15.90 \text{ MW/m}^2 & Q_3 = 16.19 \text{ MW/m}^2 \\ \Delta T_{w1} = 103.9^\circ\text{C} & \Delta T_{w2} = 105.6^\circ\text{C} & \Delta T_{w3} = 107.1^\circ\text{C} \end{array}$$

I.3. If there is no oxide film, $T_{w/\phi} = T_{\phi/c} = (T_S)_O - (\Delta T_w)_O$:

$$T_{w/\phi 1} = 138.3^\circ\text{C} \quad T_{w/\phi 2} = 148.0^\circ\text{C} \quad T_{w/\phi 3} = 157.7^\circ\text{C}$$

(Here is a significant point of comparison: for these specimen positions, HEATING5 computes 138.6, 148.4, and 158.1°C, respectively.)

I.4. Using the approximate equation for T_C :

$$T_{C1} = 69.2^\circ\text{C} \quad T_{C2} = 77.5^\circ\text{C} \quad T_{C3} = 85.8^\circ\text{C}$$

I.5. If no oxide film is present, the water-side heat transfer coefficient can be calculated directly:

$$h_1 = 0.226 \text{ MW/m}^2 \cdot \text{K} \quad h_2 = 0.226 \text{ MW/m}^2 \cdot \text{K} \quad h_3 = 0.225 \text{ MW/m}^2 \cdot \text{K}$$

(This is a comparison point of sorts: an "initial" film 0.1 μm in thickness, supporting a ΔT_ϕ of almost 1°C , was assigned in the HEATING5 computation in addition to an average $h = 0.227 \text{ MW/m}^2 \cdot \text{K}$.)

II.1. For $t > 0$, "measure" T_S [see Fig. 3, from computer output]:

$$T_{S1} = 280.4^\circ\text{C} \quad T_{S2} = 320.7^\circ\text{C} \quad T_{S3} = 375.1^\circ\text{C}$$

II.2. On the basis of these temperatures, we calculate:

$$\begin{aligned} \rho_1 &= 6.98 \times 10^{-8} \text{ } \Omega\text{-m} & \rho_2 &= 7.43 \times 10^{-8} \text{ } \Omega\text{-m} & \rho_3 &= 8.03 \times 10^{-8} \text{ } \Omega\text{-m} \\ k_{w1} &= 189.6 \text{ W/m}\cdot\text{K} & k_{w2} &= 191.1 \text{ W/m}\cdot\text{K} & k_{w3} &= 191.7 \text{ W/m}\cdot\text{K} \\ \bar{\rho} &= 7.48 \times 10^{-8} \text{ } \Omega\text{-m} \\ Q_1 &= 14.84 \text{ MW/m}^2 & Q_2 &= 15.79 \text{ MW/m}^2 & Q_3 &= 17.07 \text{ MW/m}^2 \\ \Delta T_{w1} &= 97.8^\circ\text{C} & \Delta T_{w2} &= 103.3^\circ\text{C} & \Delta T_{w3} &= 111.3^\circ\text{C} \end{aligned}$$

II.3. The temperature drops across the oxide film are calculated according to the previously noted sets of assumptions a, b, and c:

$$T_{w/\phi 1} = 182.6^\circ\text{C} \quad T_{w/\phi 2} = 217.4^\circ\text{C} \quad T_{w/\phi 3} = 263.8^\circ\text{C}$$

$$\begin{aligned} \text{a. for } \Delta T_\phi &= T_S - QX_w/2k_w - T_C - Q/h: \\ \Delta T_{\phi 1} &= 47.7^\circ\text{C} & \Delta T_{\phi 2} &= 70.0^\circ\text{C} & \Delta T_{\phi 3} &= 102.1^\circ\text{C} \\ \text{b. for } \Delta T_\phi &= [T_S - QX_w/2k_w] - [(T_S)_O - (QX_w/2k_w)_O] \\ \Delta T_{\phi 1} &= 44.3^\circ\text{C} & \Delta T_{\phi 2} &= 69.4^\circ\text{C} & \Delta T_{\phi 3} &= 106.1^\circ\text{C} \\ \text{c. for } \Delta T_\phi &= T_S - (T_S)_O \\ \Delta T_{\phi 1} &= 38.2^\circ\text{C} & \Delta T_{\phi 2} &= 67.1^\circ\text{C} & \Delta T_{\phi 3} &= 110.3^\circ\text{C} \end{aligned}$$

The calculated value of ΔT_ϕ is involved directly in the evaluation of the extent of corrosion product buildup and in the determination of its thermal conductivity k_ϕ . The comparisons of the computer values and those determined above by the three approximate equations are given in Table 1.

Table 1. Comparison of ΔT_{ϕ} values for model test specimen

Calculation basis	Temperature drop across oxide film ($^{\circ}\text{C}$)		
	ΔT_{ϕ_1}	ΔT_{ϕ_2}	ΔT_{ϕ_3}
HEATING5	48.3	71.3	105.6
Assumption II.3.a	47.7	70.0	102.1
Assumption II.3.b	44.3	69.4	106.1
Assumption II.3.c	38.2	67.1	110.3

CONCLUSIONS

The range of values calculated for ΔT_{ϕ} clearly indicates the need for care in performing calculations based on data of the type presented here. While comparisons with the computer-generated values suggest that the variations in Q and k_w need to be considered, it should be remembered that these values are also not exact. In addition, the calculations indicate that at a point near the center of the specimen, where the heat flux remains closest to the average value, the approximate calculations are most accurate or at least show best agreement with HEATING5.

On the whole, assumption II.3.a appears to give the best results for the ΔT_{ϕ} quantity, although assumption II.3.b is attractive because it is independent of h , the water-side heat transfer coefficient. Assumption II.3.c appears to be accurate only under conditions where the temperature and property changes along the specimen axis are small. However, the value of $T_s - (T_s)_0$ at each thermocouple position is a convenient method to gage the corrosion product buildup in a semiquantitative manner.

The comparisons presented here also point out that for situations where the temperature gradient along the axis of the specimen is large, the temperature at the oxide-coolant interface $T_{\phi/c}$ at each thermocouple position may not be independent of time. Additional calculations (including better assignments of the heat transfer coefficient h) will be required to see if this variation is real and if it should be considered in correlating the kinetic data.

ACKNOWLEDGMENTS

The authors are indebted to D. L. McElroy and R. E. Clausing for reviewing the manuscript and providing numerous comments. Discussions with J. C. Griess were particularly valuable.

REFERENCES

1. J. C. Griess et al., *Effect of Heat Flux on the Corrosion of Aluminum by Water. Part III. Final Report on Tests Relative to the High-Flux Isotope Reactor*, ORNL-3230, October 1961.
2. W. D. Turner, D. C. Elrod, and I. I. Siman-Tov, *HEATING5 - An IBM 360 Heat Conduction Program*, ORNL/CDS/TM-15, March 1977.
3. R. P. Tye, R. W. Hayden, and S. C. Spinney, "Thermal Conductivity of Selected Alloys at Low Temperatures," *Ad. Cyro. Eng.* **22**, 136 (1977).
4. J. C. Griess, H. C. Savage, and J. L. English, *Effect of Heat Flux on the Corrosion of Aluminum by Water. Part IV. Tests Relative to the Advanced Test Reactor and Correlation with Previous Results*, ORNL-3541, February 1976.

INTERNAL DISTRIBUTION

- | | |
|------------------------------------|---------------------------------|
| 1-2. Central Research Library | 32. B. H. Montgomery |
| 3. Document Reference Section | 33. R. M. Moon, Jr. |
| 4-5. Laboratory Records Department | 34. F. R. Mynatt |
| 6. Laboratory Records, ORNL RC | 35. A. R. Olsen |
| 7. ORNL Patent Section | 36-45. R. E. Pawel |
| 8. R. G. Alsmiller, Jr. | 46. F. J. Peretz |
| 9. S. P. Baker | 47. W. H. Power |
| 10. R. L. Beatty | 48. M. A. Schmidt |
| 11. A. Bleier | 49. D. L. Selby |
| 12. E. E. Bloom | 50. G. M. Slaughter |
| 13. C. R. Brinkman | 51. J. O. Stiegler |
| 14. R. A. Buhl | 52. P. B. Thompson |
| 15. R. E. Clausing | 53-55. P. T. Thornton |
| 16. G. L. Copeland | 56. P. F. Tortorelli |
| 17. D. F. Craig | 57. J. R. Weir, Jr |
| 18. J. H. DeVan | 58. C. D. West |
| 19. J. R. DiStefano | 59. M. K. Wilkinson |
| 20. C. V. Dodd | 60. J. M. Williams |
| 21. K. Farrell | 61. D. F. Wilson |
| 22. W. R. Gambill | 62-66. D. W. Yarbrough |
| 23. M. L. Grossbeck | 67. G. L. Yoder, Jr |
| 24. R. M. Harrington | 68. A. Zucker |
| 25. L. L. Horton | 69. H. D. Brody (Consultant) |
| 26. J. F. King | 70. G. Y. Chin (Consultant) |
| 27. J. R. Keiser | 71. F. F. Lange (Consultant) |
| 28. D. B. Lloyd | 72. W. D. Nix (Consultant) |
| 29. W. L. Marshall, Jr. | 73. D. P. Pope (Consultant) |
| 30. D. L. McElroy | 74. E. R. Thompson (Consultant) |
| 31. M. T. McFee | |

EXTERNAL DISTRIBUTION

75. DOE, OAK RIDGE OPERATIONS OFFICE, P.O. Box E, Oak Ridge, TN 37831
Office of Assistant Manager for Energy Research and
Development.
- 76-105. DOE, TECHNICAL INFORMATION CENTER, Office of Information Services,
P.O. Box 62, Oak Ridge, TN 38731
(For distribution by microfiche as shown in DOE/TIC-4500,
Distribution Category UC-2)

